The simultaneous measurement of optical activity and circular dichroism in birefringent linearly dichroic crystal sections. I. Introduction and description of the method



1990 J. Phys.: Condens. Matter 2 6807

(http://iopscience.iop.org/0953-8984/2/32/012)

J. Phys.: Condens. Matter 2 (1990) 6807–6836. Printed in the UK

# The simultaneous measurement of optical activity and circular dichroism in birefringent linearly dichroic crystal sections: I. Introduction and description of the method

J R L Moxon and A R Renshaw
Clarendon Laboratory, Parks Road, Oxford OX1 3PU, UK

Received 31 August 1989

**Abstract.** The 'HAUP' method, described by Kobayashi and Uesu, for the measurement of optical activity in birefringent crystals is extended to include dichroic effects and analysed qualitatively in a novel way using intensity contour maps. The elimination of the parasitic ellipticities of the polariser and analyser is achieved by repeating the measurement in a second crystal setting, rather than physically exchanging the prisms, which has been reported as unworkable.

## 1. Introduction

There has been a renewed interest in understanding optical rotatory dispersion (ORD) and circular dichroism (CD) in solids, especially in new inorganic electro-optic materials, for two reasons: firstly because of the relationship between these effects and electronic polarisability (Reijnhart 1970, Glazer and Stadnicka 1986, Devarajan and Glazer 1986); and secondly because of a fundamental interest in wave propagation in anisotropic and bi-anisotropic chiral media (Lakhtakia 1985, Puri and Birman 1981, Kong 1974) and the phenomenological description of the frequency and spatial dispersion of the dielectric tensor (Eimerl (1988), following Voigt (1903, 1905), Wever (1920), Szivessy and Münster (1934)). These latter studies have been particularly concerned with propagation in the presence of both linear and circular differential wave optic parameters.

Measuring optical activity and circular dichroism in birefringent linearly dichroic sections is difficult because the linear birefringence is typically 1000× larger than either of the circular effects. In terms of superposition principles, this means that the introduction of a circular birefringence into an otherwise purely linear birefringence causes the two linear eigen-modes to become very slightly elliptical. The introduction of circular dichroism causes these two modes to depart from mutual orthogonality. The effects of linear dichroism, crystal imperfections, surface roughness, instrumental setting errors, polariser and compensator errors, finite bandwidth and beam divergence all contribute to further systematic errors. It is no surprise therefore that the earliest attempts at measurement of optical activity in a birefringent crystal section (Beaulard 1893, Szivessy and Schweers 1929) failed to obtain a consistent value for the ellipticity, and relatively

0953-8984/90/326807 + 30 $03.50  

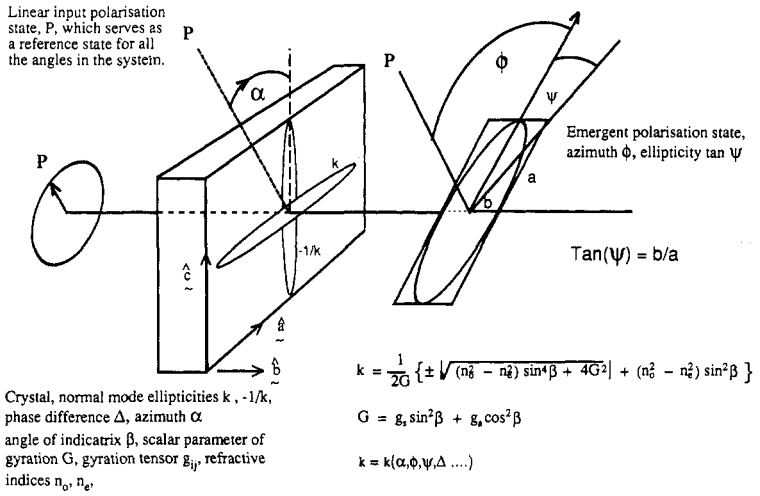


**Figure 1.** The basic polarimetry experiment on an elliptically birefringent sample using the notation of Szivessy and Münster (1934).

few subsequent papers have analysed the effects of imperfect optical components, detection systems or mechanical calibration.

In this paper we calculate the effects of linear and circular birefringence (LB, CB), and linear and circular dichroism (LD, CD), in a polariser–specimen–analyser (PSA) photometric polarimeter with imperfect components, and show how these effects can be measured. We plan to present following papers discussing experimental applications.

In order to understand the concepts underlying our method, we first review some of the earlier work.

### *1.1. Optical activity*

*1.1.1. Szivessy and Münster (1934).* The basis of all methods for measuring the optical activity in birefringent sections is to infer the ellipticity of the normal waves, $\boldsymbol{k}$, from the polarisation state of the beam emergent from the crystal, and relate this to the scalar parameter of gyration. The geometry and notation of Szivessy and Münster are shown in figure 1.

Before the advent of reliable linear electrophotometry, null methods (in which instrument settings that minimise the transmitted intensity are sought) were the only viable technique. Hence Szivessy and Münster analysed the emergent beam using a modified Sénarmont method (Ramachandran and Ramaseshan 1961). $\boldsymbol{k}$ was then derived from expressions relating these settings to $\boldsymbol{k}$ as a function of $\alpha$ and $\beta$. ($\beta$ is the orientation of the indicatrix relative to the propagation direction.) They focussed attention on three 'special' values of $\alpha$ that give rise to emergent states that can be particularly easily identified by null polarimetry. Diagrams of these settings are shown in figure 2, and the equations that relate them to $\boldsymbol{k}$ and $\Delta$ are indicated in table 1.

Szivessy and Münster proposed various methods for getting $\boldsymbol{k}$, each of which has special advantages at different values of $\alpha$ and $\beta$. The methods fall into two groups; one in which $\Delta$, the phase difference was measured externally by a compensator, and one in which it was determined implicitly by the simultaneous determination of two of the

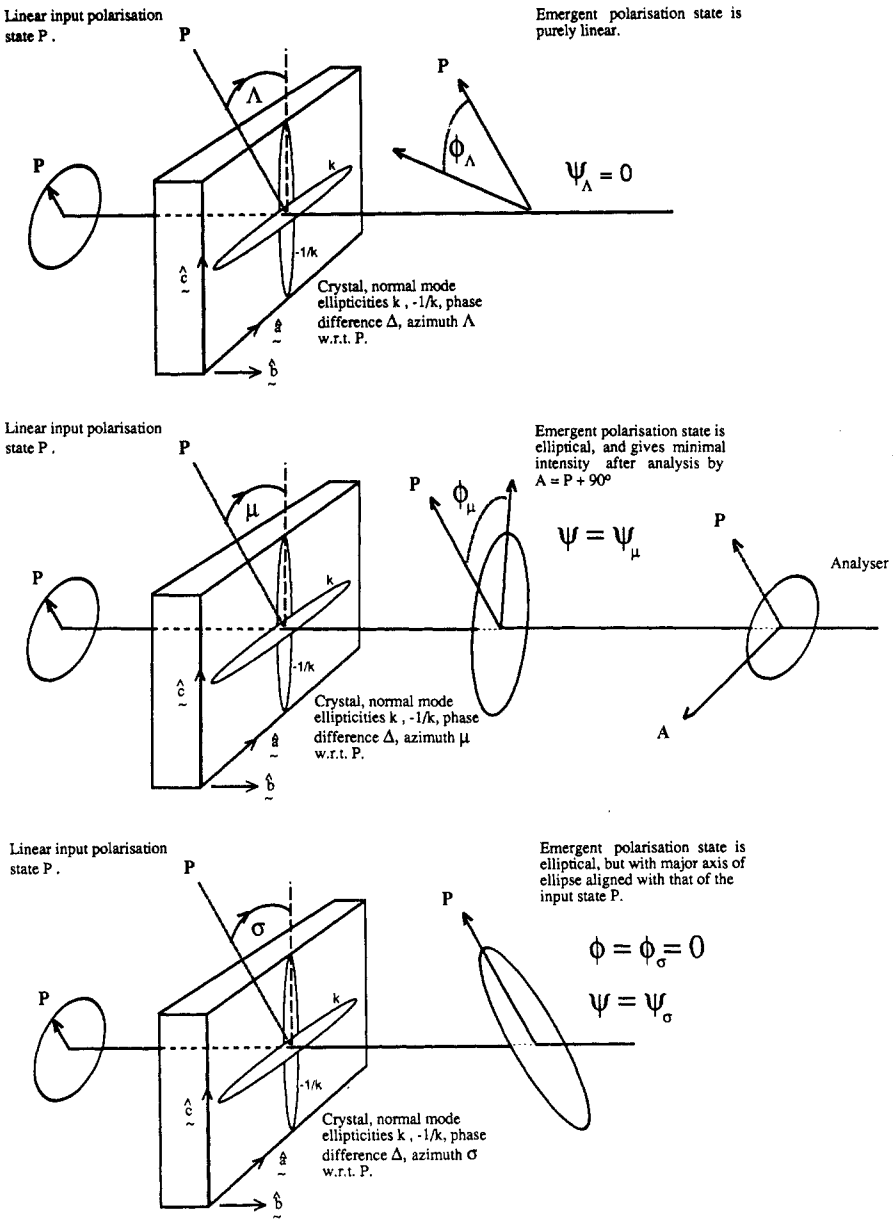


**Figure 2.** Diagrams showing the apparatus configuration for the three special settings in Szivessy and Münster (1934)—the upper, middle and lower panels show the linear, minimal and symmetry azimuths respectively.

special azimuths, and their corresponding output states. In each case they derived an expression for $k$ in terms of the value of the special azimuth concerned, or in terms of the azimuth and ellipticity of the corresponding emergent state. For example, the expression for the 'linear azimuth' $\Lambda$ was inverted particularly easily to give

$$k = (\tan \Delta/2 \pm \sqrt{\tan^2\Delta/2 - \tan^2 2\Lambda})/\tan 2\Lambda.$$

**Table 1.** The special crystal settings of Szivessy and Münster (1934).

| Azimuth | Description | Value | Characterisation of emergent state |
|---|---|---|---|
| Linear azimuth: $\Lambda$ | The four crystal azimuths for which the emergent beam is in a linear polarisation state | $\tan(2\Lambda) = \dfrac{2k}{1+k^2}\tan\dfrac{\Delta}{2}$ | $\sin(\varphi_\Lambda) = \pm\sin(2\Lambda)$ |
| Symmetry azimuth: $\sigma$ | The crystal azimuth for which the axes of the state emerging from the crystal are aligned with the vibration direction of the polariser. | $\sin(4\sigma) = -\dfrac{4k(1+k^2)}{(1-k^2)^2}\cot\dfrac{\Delta}{2}$ | $\tan(\psi_\sigma) = \left(\dfrac{4\sin^2(\Delta/2)[k^2+(1-k^2)^2\sin^2\sigma\cos^2\sigma]}{(1+k^2)^2 - 4\sin^2(\Delta/2)[k^2+(1-k^2)^2\sin^2\sigma\cos^2\sigma]}\right)^{1/2}$ |
| Minimal azimuth: $\mu$ | The four crystal azimuths that null between crossed polars | $\mu = 0$ | $\tan(2\varphi_\mu) = \dfrac{2k(1+k^2)\sin\Delta}{(1-k^2)^2 + 4k^2\cos\Delta}$ |
| | | | $\sin(2\varphi_\mu) = \pm\dfrac{4k(1-k^2)}{(1+k^2)^2}\sin^2\dfrac{\Delta}{2}$ |

Some of the methods lost the sign of $\boldsymbol{k}$, and hence could only be used to derive its magnitude. They listed five workable methods, discarding those that have an inherently low sensitivity for $\boldsymbol{k}$.

Using an externally measured $\Delta$ and one azimuth:

| Measured quantities | Derived quantity |
|---|---|
| $(\Lambda, \Delta)$ | $k$ |
| $(\sigma, \Delta)$ | $k$ |

Using two azimuths:

| Measured quantities | Derived quantity |
|---|---|
| $(\sigma, \Lambda)$ | $\|k\|$ |
| $(\sigma, \psi_\sigma)$ | $\|k\|$ |
| $(\varphi, \psi_\sigma)$ | $k$ |

All the other measurement methods could be related to this framework; below we shall make a graphical comparison of the most important, indicating the role of these special crystal settings.

*1.1.2. Bruhat and Grivet (1935).* Bruhat and Grivet used the $(\varphi, \psi_\sigma)$ method of Szivessy and Münster with the help of newer technology in the form of a photomultiplier tube and an electrically modulated version of the half-shade. Besides corroborating Szivessy and Münster's results, they were able to explain the previous failure of Szivessy and Schweers and Beaulard as being caused by errors in the determination of $\Delta$ due to too large a bandwidth in the light source. Bruhat and Grivet rejected Szivessy and Schweer's explanation in terms of beam divergence and sample misalignment, and performed calculations to show that they could not cause errors of the order of magnitude of those actually encountered, and so introduced a much more quantitative treatment of the many systematic errors besetting such experiments. They did not however discuss the effects of errors in the vital optical components of their apparatus. They noted that the theories of Voigt predicted a $1/\lambda^2$ dispersion law for the optical activity even in a birefringent section, and so made a particular point of taking measurements from 250 nm in the ultraviolet through the visible range using the many lines of a Mercury vapour lamp. They also noted that an electronic detection system could in principle be used to make a photometric determination of the optical activity. They gave expressions to show how $\boldsymbol{k}$ could be derived from least-squares refinement of the intensity as a function of various angles in the system. However, they rejected the technique because of the limits of their detection system. This idea was explicitly taken up by Kobayashi and Uesu (1983).

*1.1.3. Konstantinova et al (1969).* Konstantinova's analysis and measurement method were reported after more than 30 years of silence in the publications. Her method was to use a new crystal azimuth which we shall call the crystallographic zero azimuth, in

which the crystal axes (and hence the principal axes of the indicatrix) were exactly aligned with the polarisation direction of the polariser. In this case, the emergent state is elliptical, and its azimuth deviates from that of the input state. Instead of *measuring* the phase, use was made of bright Hg or Xe broad-band high-pressure arc lamps, and an automatically controlled grating monochromator to scan the wavelength, thus 'washing out' the phase dependency, and revealing a fringe pattern dependent on the order of the crystal. The azimuth of the emergent state oscillates about that of the input state with $\Delta$, and is given by an expression very similar to that of the linear azimuth $\Lambda$ of Szivessy and Münster:

$$\tan(2\varphi) \simeq -2k \sin(\Delta) \qquad \tan(\psi) \simeq \mp k(1 - \cos(\Delta)).$$

The alignment was not attempted by x-ray methods, but simply by adjusting the crystal azimuth until these oscillations with phase were evenly distributed about the zero position when the wavelength was scanned. Because the system was self-aligning, little attention was paid to errors in the optical components. However, the authors made a seminal observation that the envelope of the dispersively decaying sine wave was noticeably different when the crystal was rotated by 90° from its original azimuth (figure 3.) They made the following observation:

> 'It is evident that the values of $\chi$ [$\varphi$ in our notation] for these cases do not coincide. Apparently this difference is connected to some kind of additional ellipticity which has not been successfully eliminated.'

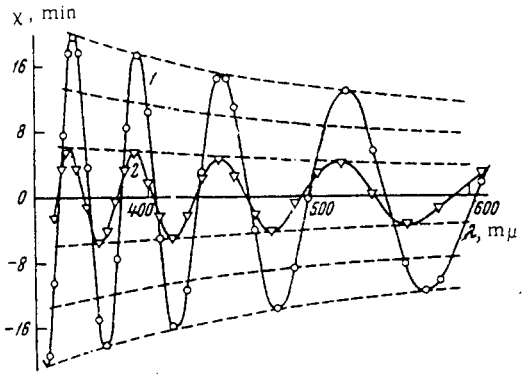


**Figure 3.** The anomalous result for the wavelength dependence of the emergent azimuth observed by Konstantinova *et al* (1969), showing a difference between the two crystal settings (separated by 90°).

Our analysis below shows that these errors are the ellipticities of the polariser and analyser, and that the different values of emergent beam azimuth for different quadrant positions of the crystal can be exactly predicted. We utilise this knowledge to eliminate their effect. Konstantinova's method has been widely used, notably by Ivanov and Konstantinova (1970), Ivanov and Chikhladze (1976), Kaminskii *et al* (1983), Okorochkov *et al* (1984), Vlokh *et al* (1986)

*1.1.4. Anderson et al (1974).* This method was the first published genuinely photometric method of optical activity determination in birefringent sections. The authors took an

expression derived by Voigt and noted by Szivessy and Münster for the transmitted intensity at the crystallographic zero azimuth:

$$J = J_0[k^2/(1 + k^2)^2] \sin^2(\Delta/2).$$

Following Konstantinova, they therefore scanned this intensity with wavelength and picked out the extreme values to show the dispersion of $k^2$. This method relies on the use of a beam splitter to correctly relate $J_0$ and $J$. Anderson *et al* obtained results for $AgGaS_2$, which has quite large ellipticity values, and did so to follow up the work of Hobden (1968), who had made a measurement at the special zero-crossing wavelength in $AgGaS_2$ at which the linear birefringence was accidentally zero. The technique was used again by Kobayashi *et al* (1978) on the more difficult sample of $\alpha$-quartz with the improved technology of a photon detection system to deal better with the very low light levels. In neither of these papers were any of the optical component and other systematic errors dealt with.

*1.1.5. Horinaka et al (1980, 1985).* The difficulty of correctly relating the measurements $J_0$ and $J$ in the above method was overcome in a modulated experiment, in which the normalisation was achieved by the division of the $2\omega$ and the $4\omega$ Fourier components. The modulator can be a rotating phase plate or electro-optic retarder. Scanning with wavelength is still necessary, however, since the $2\omega$ signal is oscillatory with phase. The good signal-to-noise ratios available in modulated experiments (Aspnes 1973, Azzam 1978) allowed these authors to move from the relatively 'easy' case of $AgGaAs_2$ in their 1980 paper ($k$ is relatively large) to the more difficult $\alpha$-quartz (Horinaka *et al* 1985), and get results that compared favourably with those of Bruhat and Grivet. Horinaka used the coherency matrix formulation in calculating the Fourier coefficients.

The coherency matrix of the transmitted beam and its intensity are:

$$\boldsymbol{\rho}_f = \mathbf{M}_A\mathbf{M}_M\mathbf{M}_S\boldsymbol{\rho}_i\mathbf{M}_S^+\mathbf{M}_M^+\mathbf{M}_A^+ \qquad I = \mathrm{Tr}(\boldsymbol{\rho}_f) = I_{2\omega} + I_{4\omega}$$

where A, M and S mean analyser, modulator and sample, respectively, and the $2\omega$ and $4\omega$ Fourier components are:

$$I_{2\omega} = I_0[k - (k^2 + \Theta^2)^{1/2} \cos(\delta + \zeta)] \sin\alpha \qquad I_{4\omega} = (I_0/2) \sin^2(\alpha/2)$$

where $\alpha$ is the phase angle of the modulator. The wavelength-averaged $2\omega$ signal is written as

$$\langle I_{2\omega}\rangle_\lambda = I_0 k \sin(\alpha)$$

leading to a sign-indeterminate value for $k$:

$$k = \tfrac{1}{4} \tan(\alpha/2)\langle I_{2\omega}\rangle_\lambda / I_{4\omega}.$$

Modulated methods had been discussed and used in both reflection and transmission ellipsometry considerably before this publication (see Aspnes 1973, Pancharatnam 1955), but it seems that Horinaka's was the first application to the measurement of optical activity in birefringent sections.

*1.1.6. Kobayashi and Uesu (1983).* This publication was important on two accounts. First, it used a suggestion of Bruhat and Grivet that *k could* be derived from least-squares refinement of the intensity as a function of various angles in the system given a linear and sensitive enough detection system. Secondly, it explicitly took into account the ellipticity errors of the polariser and analyser, suggesting that these alone could completely mask the normal-mode ellipticity sought. Kobayashi *et al* made the important

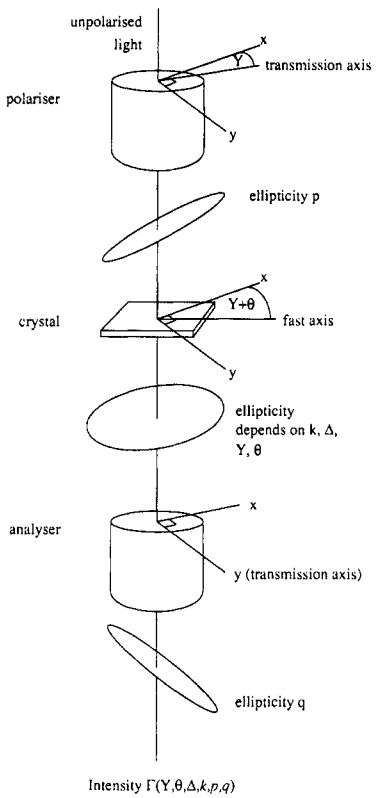


**Figure 4.** The definition of the angles Y and $\theta$, and the errors $p$ and $q$ in the HAUP experiment of Kobayashi and Uesu (1983).

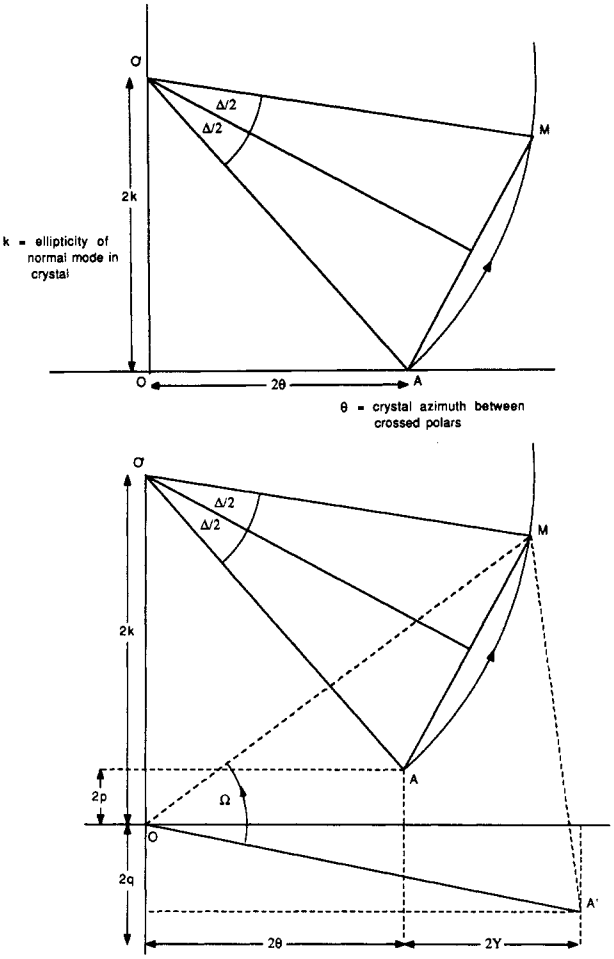


**Figure 5.** The upper panel shows the Poincaré diagram for Bruhat and Grivet's photometric calculation, in which the final intensity depends on the arc AM, and the lower panel shows how this plane-geometric approximation is modified in the Kobayashi analysis by the introduction of the polariser and analyser errors and a general analyser angle. The intensity now depends on the arc A'M.

observation that, if such errors must be taken into the analysis in order to eliminate them somehow, then the number of extra components, such as modulators, beam splitters, windows, and compensators, had to be kept to an absolute minimum, for *computational* reasons. The authors also followed Bruhat and Grivet in using a plane-geometric approximation on a small area of the Poincaré sphere. Figure 4 indicates their coordinate system; figure 5 shows the spherical trigonometric basis of Kobayashi's adaptation of Bruhat and Grivet's calculation leading to a bi-quadratic expression for the intensity in the angles Y and $\theta$:

$$\Gamma(\theta, \mathrm{Y}, p, q) = A(\theta, p, q) + B(\theta, p, q)\mathrm{Y} + \mathrm{Y}^2$$

(where $A$, $B$ are both quadratic in $\theta$).

They collected the intensity data in Y-strips to find $B$ as a function of $\theta'$. $\theta' = 0$ is at Szivessy and Münster's minimal azimuth. This transformation has the effect of grouping the $p$ and $q$ error terms into occurrences of $\gamma = (p - q)$, which can be eliminated in principle by physically exchanging the polariser and analyser and repeating the experiment. Since

$$B(\theta', p, q) = -(2k - \gamma)\sin(\Delta) + 4\sin^2(\Delta/2)\theta'$$

defines a straight line, the normal-mode ellipticity, $k$, can be extracted from the intercept in conjunction with a knowledge of $\Delta$ extracted from the gradient. This technique, with various modifications, has been applied successfully by Kobayashi *et al* (1983, 1984, 1985, 1986a, 1987, 1988) and Saito *et al* (1985, 1987).

### *1.2. Circular dichroism*

The corresponding difficulties in measuring circular dichroism in birefringent sections, and in the presence of other optical effects, have been investigated much more recently. The circular dichroism, while defined as a difference in absorption coefficients for circular reference states, does have an effect on the polarisation states of the normal waves in the crystal (causing the major axes of the elliptical states to depart slightly from mutual orthogonality, and their ellipticities to diverge). Hence the effect *could* be determined polarimetrically, as we shall show below, and determined along with the optical activity and other effects. However, the main attempts at these measurements have been performed using the modulating dichrograph routinely used in chemical analysis of liquids and gases. Here the difference in absorption itself is measured by switching rapidly between R and L polarisation and Fourier analysing the resulting signal.

*1.2.1. Castaño (1969)* observed that for some of the non-centrosymmetric point groups, rotational tensor averages do not disappear. He therefore compared the results for optic axis dichroism with those for a powder sample, and knowing the relationship of the tensor average to the two independent components in the particular case, was able to infer the component of circular dichroism perpendicular to the optic axis. The technique, however, is not general, since it relies on a relationship that is only true for certain of the optically active point groups.

*1.2.2. Perekalina et al (1977)* worked on the single-crystal experiment and addressed the problem of exactly what goes wrong in the operation of a normal modulated dichrograph if the sample is a birefringent single-crystal section. The problem arises because of the sinusoidal modulation between the R and L states. As soon as there is any net linear component to the incident polarisation state (as the electro-optic modulator is switching), then the wave optics in the crystal differ from the linearly isotropic case, and the Fourier components in the final signal are altered. They proposed modifications to both the instrument and the interpretation of the data in order to extract the true value of the CD.

*1.2.3. Baturin et al (1983)* noted that even the optical rotation, which would always occur together with the dichroism, and would begin to have significant values away from the centre of the dichroism band, causes similar errors in modulated dichrograph operation.

It seems therefore that the polarimetric approach to circular dichroism has not yet been investigated.

### *1.3. Linear dichroism*

Most transparent birefringent materials are deemed to be 'non-linearly dichroic' and a common criterion, especially in the mineralogical literature, is simply visible pleochroism. Several of the purely theoretical papers (Konstantinova *et al* 1969, Grechushnikov *et al* 1980) derived the linear dichroism terms, but only in very few papers do we find mention of the need to take them into account in particular experiments. Baturina *et al* (1985) noted that all crystal imperfections and surface roughness will give an apparent linear dichroism, and appear to affect the intrinsic wave optics of the specimen. Chetkin *et al* (1979) noted the problem in Faraday effect measurement in orthoferrites and we consider it important to include it in our own analysis.

### *1.4. Integrated or universal techniques*

Simultaneous extraction of all the differential wave optical effects has been considered by Raab (1982), in a purely theoretical paper, along the lines of a generalised version of the dichrograph experiment. He proposed a number of pairs of related input and analyser polarisation states from which to measure intensity differentials. The approach is difficult for a number of reasons, not least because of the need for wavelength-independent circular polarisers and analysers. Henty and Jerrard (1976) claimed the development of a 'universal' ellipsometer and used it to make simultaneous measurements of ORD and CD in dextrorotatory tris-(ethylenediamine) cobalt III iodide monohydrate. They used Faraday modulation and a split emergent beam with two separate analysing units; however, the apparatus was designed for *isotropic* media only and so would not function in birefringent crystal sections without considerable adaptation.

We will now develop our 'universal' treatment from Kobayashi's analysis. Insights into the role of various systematic errors and other wave-optical effects are then applied to the modulated technique of Horinaka *et al* (1980, 1985).

## 2. Calculations for the transmitted intensity

We have used the Jones (1948) calculus, and, following Wyant (1981), a symbolic algebra system (Hearn 1985) for all our calculations, and so we make a variety of controlled approximations. The basic premise of the Jones method is that an input polarisation state, represented by a column vector $\boldsymbol{J}_i$, is mapped into an output state $\boldsymbol{J}_f$ by a $2 \times 2$ matrix called the **M** matrix for the system. The four coefficients of **M** may each be complex, so there are a total of eight parameters that describe the crystal as an optical system. Six of these parameters may be chosen according to table 2. The remaining two parameters describe the orientation of the crystal relative to the coordinate axes. For a completely general 'optical black box', or a biaxial crystal, two angles would be needed: one to locate the special directions for linear birefringence, and one for the corresponding special directions for linear dichroism. In a uniaxial crystal, symmetry demands that these special directions coincide, and so the orientation of the crystal is described by just one angle—the angle the fast axis makes with the $x$ direction.

**Table 2.** Wave-optic parameters following Jones (1948). Note that the $\delta$ used here is half of that used by Nye (1985). Jones originally defined $\rho$ as positive for laevo-rotatory crystals, contrary to the current widely accepted definition followed here.

| Effect | Description | Definition |
|---|---|---|
| Refraction | $n$ is the (real part of the) mean of the refractive indices of the two eigenmodes | $\eta = \frac{2\pi}{\lambda} n$ |
| Absorption | $k$ is the mean extinction coefficient (imaginary part of the mean refractive index) | $\kappa = \frac{2\pi}{\lambda} k$ |
| Linear birefringence | $n_y - n_x$ is the difference between the principal refractive indices for linear polarisation states | $\delta = \frac{\pi}{\lambda}(n_y - n_x)$ |
| Linear dichroism | $k_y - k_x$ is the difference between the principal extinction coefficients for linear polarisation states | $\varepsilon = \frac{\pi}{\lambda}(k_y - k_x)$ |
| Circular birefringence (optical activity) | $n_L - n_R$ is the circular birefringence (positive for dextro-rotatory crystals) | $\rho = \frac{\pi}{\lambda}(n_L - n_R)$ |
| Circular dichroism | $k_L - k_R$ is the difference between the extinction coefficients for L and R circularly polarised light | $\sigma = \frac{\pi}{\lambda}(k_L - k_R)$ |

### *2.1. The form of the* **M** *matrix for some special cases*

The general form of the **M** matrix when the $x$ axis is coincident with the fast axis in a (uniaxial) crystal is

$$\mathbf{M} = e^{(-\kappa - i\eta)z} \begin{bmatrix} \cosh Qz + [(\varepsilon + i\delta)/Q] \sinh Qz & [(\rho + i\sigma)/Q] \sinh Qz \\ [-(\rho + i\sigma)/Q] \sinh Qz & \cosh Qz - [(\varepsilon + i\delta)/Q] \sinh Qz \end{bmatrix}$$

where $Q^2 = (\varepsilon + i\delta)^2 - (\rho + i\sigma)^2$ and $z$ is the crystal thickness.

When there is no dichroism, the quantity $Q$ is wholly imaginary and the matrix **M** takes the simple form.

$$\mathbf{M} = e^{(-\kappa - i\eta)z} \begin{bmatrix} \cos \varphi z + i \sin \varphi z & (\rho/\delta) \sin \varphi z \\ (\rho/\delta) \sin \varphi z & \cos \varphi z - i \sin \varphi z \end{bmatrix}$$

where $\varphi = \sqrt{\delta^2 + \rho^2}$. This describes a birefringent, optically active crystal in which the normal modes are orthogonal and have ellipticity $k = \rho/2\delta$. In order to produce a simple form for **M** in the dichroic case it is necessary to make some assumptions about the relative sizes of $\delta$, $\varepsilon$, $\rho$ and $\sigma$. When the linear birefringence is the dominant effect, we may ignore terms of order $(\varepsilon/\delta)^2$, $(\rho/\delta)^2$ and $(\sigma/\delta)^2$. This is the usual situation, although there are examples of materials and crystal directions where this is not true, in which case the analysis must proceed with different approximations. In the above approximation the quantity $Q$ is given by

$$Q = \sqrt{(\varepsilon + i\delta)^2 - (\rho + i\sigma)^2} \simeq \varepsilon + i\delta.$$

We make the further approximation that the quantity $\varepsilon z$ is small, so that $\cosh(\varepsilon z) \simeq 1$ and $\sinh(\varepsilon z) \simeq \varepsilon z$. At this stage it is convenient to introduce a new set of parameters defined by the relations

$$k = \tfrac{1}{2}\rho/\delta \qquad k' = \tfrac{1}{2}\sigma/\delta \qquad \Delta = 2\delta z \qquad E = 2\varepsilon z.$$

Here $\Delta$ is the difference in phase and $E$ the difference in amplitude between the normal modes after the beam has passed through the crystal. In this approximation $\Delta$ is due solely to the linear birefringence, and $E$ to the linear dichroism. The parameters $k$ and $k'$ describe the optical rotation and circular dichroism. In the absence of linear dichroism $k + \mathrm{i}k'$ is the ellipticity of the (non-orthogonal if $k' \neq 0$) normal modes, but in a linearly dichroic crystal this ellipticity also depends on $\varepsilon$, and $k$ and $k'$ do not have a simple meaning.

Note that in the convention of Jones (1948), $\delta$ is always positive (even for crystals with a negative birefringence) and hence the sign of $\rho$ is given by the sign of $k$.

The matrix **M** can now be written as

$$\mathbf{M} = \mathrm{e}^{(-\kappa - \mathrm{i}\eta)z} \begin{bmatrix} \left(1+\frac{E}{2}\right)\left(\cos\frac{\Delta}{2}+\mathrm{i}\sin\frac{\Delta}{2}\right) & 2(k+\mathrm{i}k')\left(\sin\frac{\Delta}{2}-\mathrm{i}\frac{E}{2}\cos\frac{\Delta}{2}\right) \\ -2(k+\mathrm{i}k')\left(\sin\frac{\Delta}{2}-\mathrm{i}\frac{E}{2}\cos\frac{\Delta}{2}\right) & \left(1-\frac{E}{2}\right)\left(\cos\frac{\Delta}{2}-\mathrm{i}\sin\frac{\Delta}{2}\right) \end{bmatrix}.$$

### 2.2. *Calculation of the intensity transmitted in a PSA system*

The above form of the **M** matrix can be used to calculate the intensity transmitted by a polariser–sample–analyser system as a function of the two independent angles in such an arrangement. For consistency with Kobayashi these angles are called Y and $\theta$ and are defined as shown in figure 4.

The light transmitted by the polariser is elliptically polarised with ellipticity $p$ and azimuth Y. It is therefore described by the Jones vector

$$\boldsymbol{J}_\mathrm{i} = \begin{bmatrix} \cos \mathrm{Y} \cos p - \mathrm{i} \sin \mathrm{Y} \sin p \\ \sin \mathrm{Y} \cos p + \mathrm{i} \cos \mathrm{Y} \sin p \end{bmatrix}.$$

The fast axis of the crystal makes an angle $\mathrm{Y} + \theta$ with the $x$ axis, and so the **M** matrix must be transformed as follows:

$$\mathbf{M}' = \mathbf{R}^\mathrm{T}(-(\mathrm{Y}+\theta))\mathbf{M}\mathbf{R}(-(\mathrm{Y}+\theta))$$

where **R** is the rotation matrix

$$\mathbf{R}(\alpha) = \begin{bmatrix} \cos\alpha & -\sin\alpha \\ \sin\alpha & \cos\alpha \end{bmatrix}.$$

The light emerging from the crystal has a Jones vector

$$\boldsymbol{J} = \mathbf{R}^\mathrm{T}(-(\mathrm{Y}+\theta))\mathbf{M}\mathbf{R}(-(\mathrm{Y}+\theta))\boldsymbol{J}_\mathrm{i}.$$

The analyser is fixed with its transmission axis along the $y$ axis and is assumed to transmit light polarised with ellipticity $q$. The appropriate **M** matrix is

$$\mathbf{M}_\mathrm{an} = \begin{bmatrix} \sin^2 q & -\mathrm{i}\sin q \cos q \\ \mathrm{i}\sin q \cos q & \cos^2 q \end{bmatrix}.$$

After the analyser, the Jones vector of the light is

$$\boldsymbol{J}_f = \mathbf{M}_{an}\boldsymbol{J}$$

and the transmitted intensity is

$$\Gamma(\Upsilon, \theta, \Delta, E, k, k', p, q) = \boldsymbol{J}_f \boldsymbol{J}_f^{\mathrm{T}}.$$

The full expression for the transmitted intensity is extremely cumbersome, especially when multiple reflections are taken into account (see below) but can be derived and manipulated using the symbolic algebra package 'Reduce' (Hearn 1985), allowing us to investigate the properties of $\Gamma$ over the whole angular region and for any combination of values of the parameters $\delta$, $\varepsilon$, $\rho$ and $\sigma$. We are not therefore tied *ab initio* to any particular approximation scheme. Furthermore, we can test fitting procedures (based on a particular approximation) by Monte Carlo simulation using data calculated from the symbolic expression (with suitable noise and other errors included).

The generalised linear least-squares method (expounded in many standard works such as Press *et al* (1986)) has the advantage that it can use a linear combination of *non-linear* functions, possibly of several variables; this allows us to use the same computer routine to make refinements using full-angle bivariate spherical trigonometric formulae, and also their polynomial approximations, to any degree. Expansions of increasingly higher degree do not necessarily mean an unmanageable number of basis functions, since terms can be grouped together to produce a linear function in the original number (say $N$) of unknown parameters. For example, in a full-angle formulation (in which, however, the smaller wave-optic parameters are linearly approximated) we can write

$$\Gamma = \Gamma \begin{bmatrix} 1 \\ \cos(4\theta + 4\Upsilon) \\ \sin(4\theta + 4\Upsilon) \\ \cos(2\theta + 2\Upsilon) \\ \sin(2\Upsilon) \\ \cos(2\Upsilon) \end{bmatrix}$$

where the 'parameters' are linear combinations of $k$, $k'$, $p$, $q$, $E$ etc. A bi-quartic approximation to the previous expression, however, can be written as

$$\Gamma = \Gamma \begin{bmatrix} 4\theta^2 - \frac{16}{3}\,\theta^4 + 4\theta\Upsilon - \frac{16}{3}\,\theta^3\Upsilon - 8\theta^2\Upsilon^2 - \frac{8}{3}\theta\Upsilon^3 \\ -\Upsilon + \frac{2}{3}\Upsilon^3 \\ \Upsilon^2 - \frac{1}{3}\Upsilon^4 \\ 4\theta^3 + 12\theta^2\Upsilon \\ 4\Upsilon^2 - 4\theta^2\Upsilon \end{bmatrix}$$

where the 'parameters' are different but determined linear combinations of the desired wave-optic and instrumental error terms.

In this case both the 'full-angle' formula and the bi-quartic refinements will rely on a $6 \times 6$ matrix inversion of the inner product of the design matrix and its transpose. Thus there is no time penalty in either experimental data processing, or in Monte Carlo simulation in using either of these models.

An outline of our least-squares program is given in Appendix 1.

In Kobayashi's 'HAUP approximation', the intensity can be expanded as a Taylor series as far as quadratic terms; this corresponds to Bruhat and Grivet's plane-geometric approximation. The transmitted intensity can be written in matrix form as

$$\Gamma(\mathrm{Y}, \theta) = (1\ \mathrm{Y}\ \mathrm{Y}^2)\,\mathbf{C}\begin{bmatrix}1\\ \theta\\ \theta^2\end{bmatrix}.$$

For a purely birefringent material, **C** has a particularly simple form:

$$\mathbf{C} = \begin{bmatrix}0 & 0 & 4\sin^2(\Delta/2)\\ 0 & 4\sin^2(\Delta/2) & 0\\ 1 & 0 & 0\end{bmatrix}.$$

Contours of constant intensity, at general phase, form ellipses in $(\mathrm{Y}, \theta)$; when $\Delta$ approaches the 'singular' values of $2n\pi$ or $(2n+1)\pi$, the ellipticity vanishes, but the azimuth assumes asymptotic values of 0 and $\tan^{-1}(2)$ respectively, measured from the Y axis.

It is appropriate at this point to indicate the general form of the function $\Gamma(\mathrm{Y}, \theta, \Delta, E, k, k', p, q)$ qualitatively by computer simulation. Since the intensity is dominated by the contribution from the linear birefringence, it is helpful to visualise the effect of the other parameters as perturbations on $\Gamma(\mathrm{Y}, \theta, \Delta)$, the surface for a purely linearly birefringent material. This will serve to illuminate the algebraic discussion that follows.

## 3. Qualitative description of wave-optic parameters and measurement methods by means of the 'HAUP map'

### *3.1. Basic 2D intensity maps for birefringent material*

Figure 6 shows the intensity contours for the bivariate function $\Gamma(\mathrm{Y}, \theta)$ (which we shall later refer to as a 'HAUP map') for a purely birefringent, non-absorbing, non-dichroic crystal as $\Delta$, the phase difference, is varied between 0 and $2\pi$.

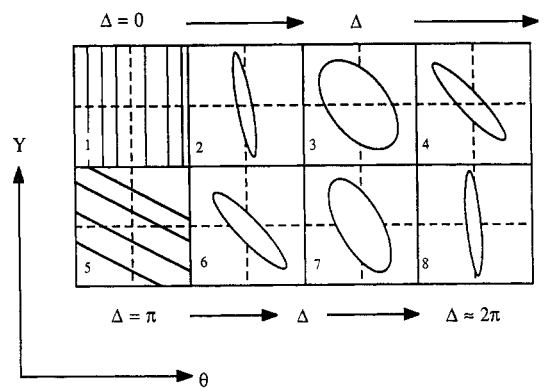


**Figure 6.** Intensity contours for the bivariate function $\Gamma(\mathrm{Y}, \theta)$ for a purely birefringent, non-absorbing, non-dichroic crystal, as $\Delta$, the phase difference, is varied between 0 and $2\pi$.

There are two special positions, at $\Delta = 2n\pi$, and at $\Delta = (2n + 1)\pi$. At $\Delta = 0$, it is as if the crystal were not present, and so the map is independent of $\theta$, and forms a vertical 'crossed-polars trough'. At $\Delta = \pi$, a more interesting singularity occurs with a trough-like feature lying at a gradient of $-\frac{1}{2}$ through the centre of the map. At other values of $\Delta$, a local elliptical minimum occurs, which rotates and changes ellipticity with phase. Our 2D refinement method, following Kobayashi and Uesu, finds $\Delta$ essentially by observing the shape, orientation and position of this ellipse. It turns out that optical activity, circular dichroism and the ellipticity of the polars only perturb the position of this minimum. The linear dichroism, multiple reflections and other effects can disturb the shape and orientation.

### *3.2. Characterisation of measurement methods in terms of HAUP maps*

In figure 7 the HAUP map for some general value of $\Delta$ is shown with Szivessy and Münster's special azimuths, and Kobayashi's $\theta_0$ which is seen to be the same as the 'minimal azimuth'. Kobayashi *et al* (1978) (following Anderson *et al* 1974) monitored $\Gamma(0, 0)$ as a function of wavelength giving a fringe sequence, with $k^2$ as an envelope. Horinaka *et al* (1980, 1985), also working at the origin, gave the modulated counterpart.

Our own approach does not depend on the location of any of the special points, but proceeds by a 2D least-squares fit to a grid of intensities covering the position of the intensity minimum.

### *3.3. Distortion of the HAUP map for linear birefringence at general phase difference $\Delta$ by circular effects and instrumental errors*

In figures 8–12 we show simulations of distortions that occur in the HAUP map of a linearly birefringent material when effects such as optical activity, circular dichroism, combinations of polariser and analyser errors, linear dichroism and multiple reflections are introduced. The +, − signs refer to a raising and lowering of the surface, and the arrows indicate linear or angular displacements of the 2D intensity minimum.

These diagrams were helpful for ascertaining optimal data collection strategies, and also in gaining a qualitative insight into the algebra; for instance, the fact that circular dichroism and instrument errors of the type $p + q$ both occur in the expression for $\theta_0$, the minimal azimuth, can be clearly seen in the similarity of their contour maps as separate effects. Errors of the type $\gamma = p - q$, however, give a contour map of deformation that is similar to that of optical activity, which relates to the occurrence of $2k - \gamma$ in the $\theta_0$-transformed intensity in Kobayashi's analysis.

In each plot we show two adjacent HAUP minima (separated by a 90° rotation of the crystal) to show that the perturbation is not always symmetrical in these two positions; for example, we can use information from both settings to eliminate $\gamma$ (since $k$ is symmetrical, and $\gamma$ anti-symmetrical in the two positions) without the need to exchange the polariser and analyser.

The basic significance of $p$ and $q$ in terms of their distortion of the optical intensity function, and their breaking of the symmetry of $\Gamma$ at the two crystal settings has been observed in a much more extreme form by Stetiu (1983) while using polaroid sheet analysers.

For large data regions, we can observe the qualitative aspects of the breakdown of the small-angle approximation for the different optical effects. One can also see the

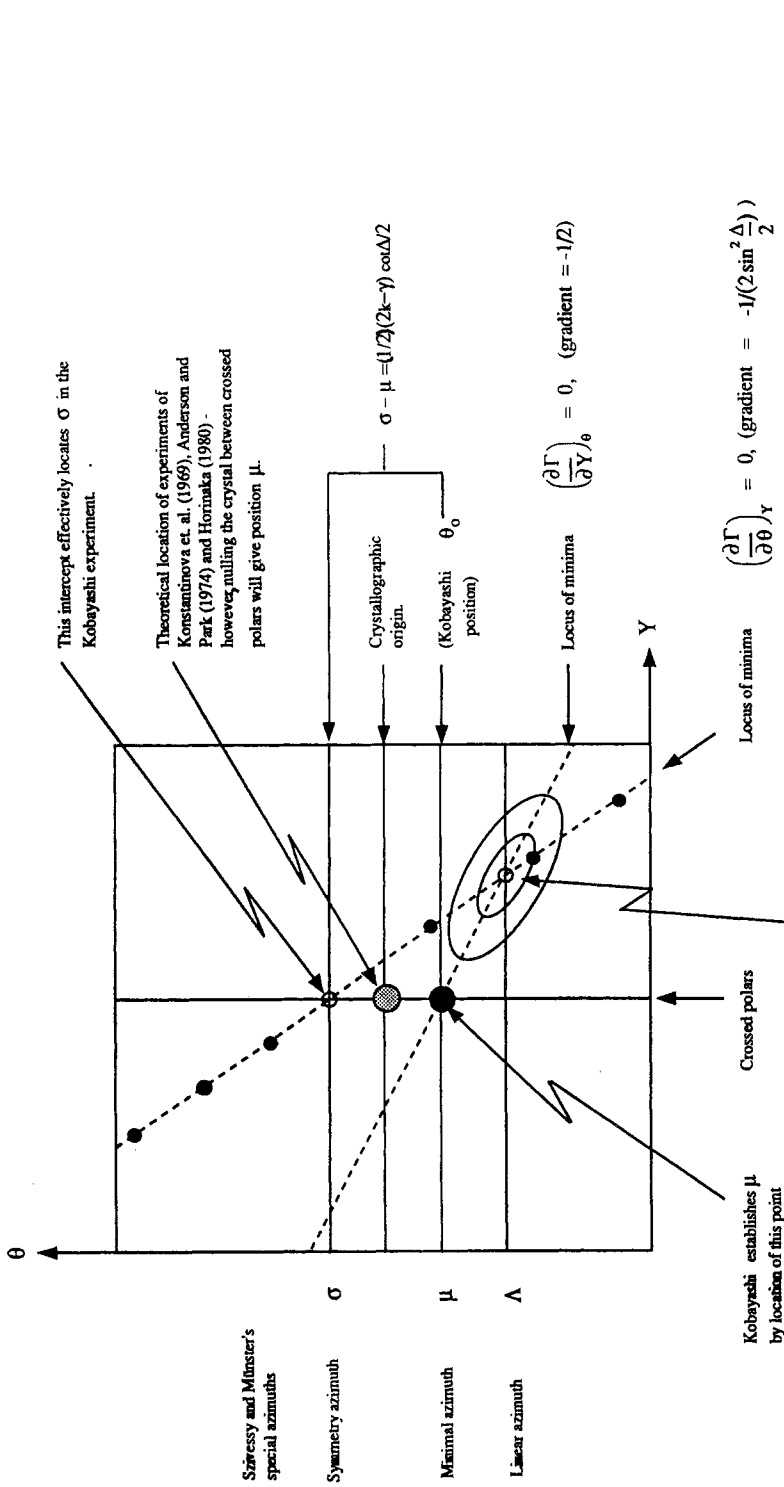


**Figure 7.** The special angles and crystal, settings of Szivessy and Müster, Horinaka *et al*, Anderson *et al*, and Kobayashi and Uesu, indicated on a 'HAUP map', a contour map of the transmitted intensity as a function of the two independent angles $Y$, $\theta$.

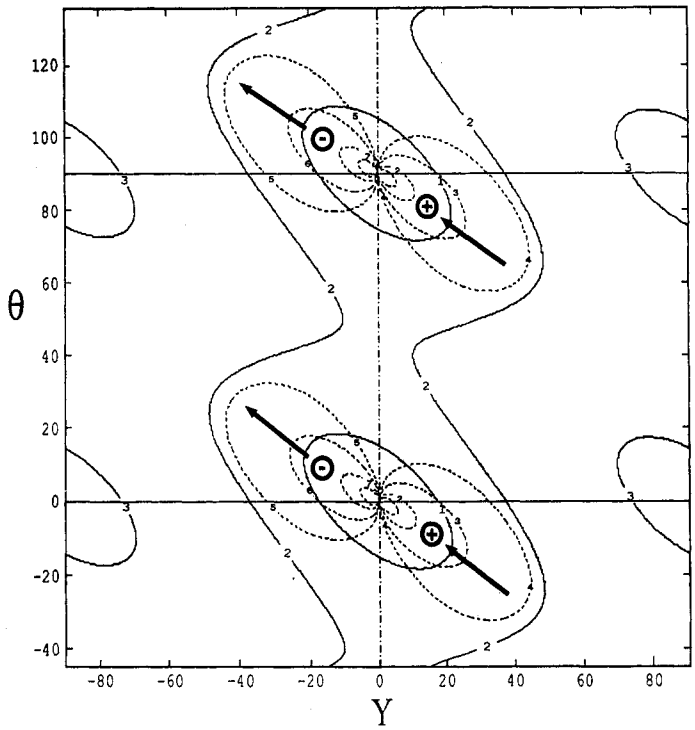


**Figure 8.** Optical activity. The 'dipolar distortion' shows the same polarity at the same position, corresponding to physical displacements of the intensity ellipses (indicated by arrows). The + and − signs indicate a raising and lowering respectively of the original surface. The contours of large fractional distortion lie in the centre of the map.

breakdown in similarities; e.g. $p + q$ and circular dichroism only give the same contour pattern in the small-angle region, but show different kinds of distortion and asymmetry between the 90° positions when the angles are much larger. This kind of information allows us to know more clearly when we must use a particularly small data region, or when we can 'get away with' a much larger one (in which case we can benefit from the higher intensities and hence shorter data collection times). We can also tell which parameters will be safely obtainable through non-linear optimisation of full-angle formulae for the intensity, the effects of which will be lost in noise as the grid size is increased (e.g. normal-mode ellipticity, $k$) and so on.

In most cases, the region of strongest distortion is at the centre of the map, and hence the use of 'small' data grids in the HAUP region is justified. The distortion patterns are 'dipolar'. In figure 12 linear dichroism shows a very different pattern (multiple reflections give a similar map), in which the contours of highest and lowest fractional distortion extend over all of $(Y, \theta)$ space; for these effects therefore it is not necessary to work within the HAUP region, with the advantage that one does not need to work at the very low flux levels near the origin; LD bands are likely to occur in regions of strong overall absorption in which we would be struggling to get realistic intensities through the instrument if we worked near the origin.

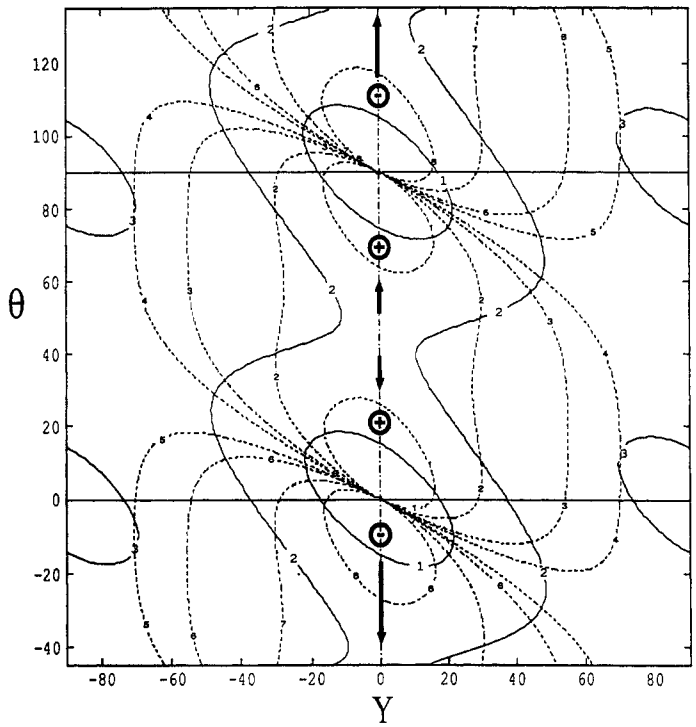


**Figure 9.** CD. The distortion is again 'dipolar', and the contours of greatest fractional distortion lie at the centre of the map. The arrows indicate a shift along the $\theta$-direction of the intensity minimum. This shift is in opposite directions for the two crystal positions.

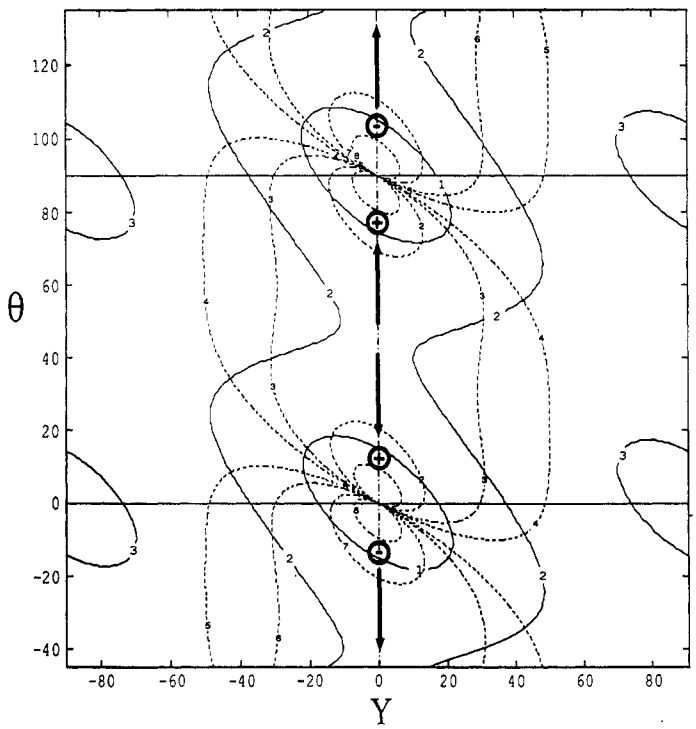


**Figure 10.** $p + q$ errors. The map is very similar to that of figure 8, a fact reflected in the way that both $p + q$ and CD occur in the expression for $\theta_0$, the minimal azimuth.

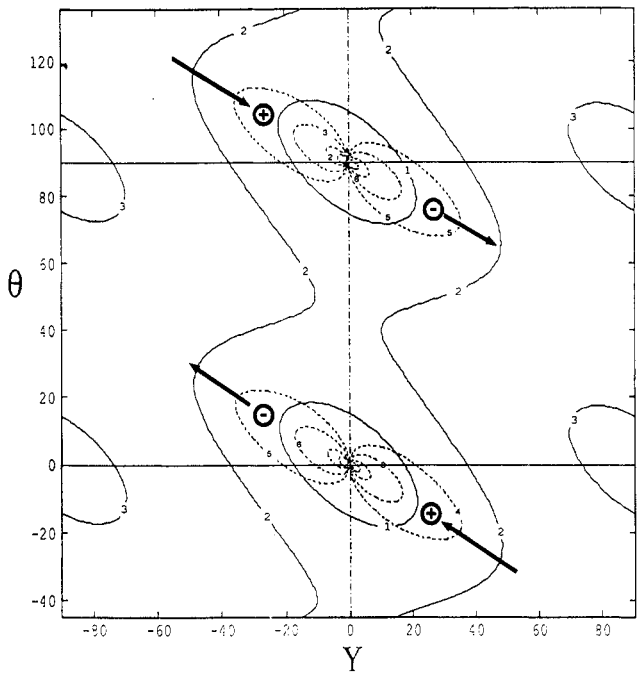


**Figure 11.** $p - q$ errors. Distortions due to errors of the form $p - q$ are similar in appearance to those from optical activity, except that these distortions are antisymmetric with respect to the two crystal positions. Hence the optical activity and $p - q$ can be separated by using grids from both positions.

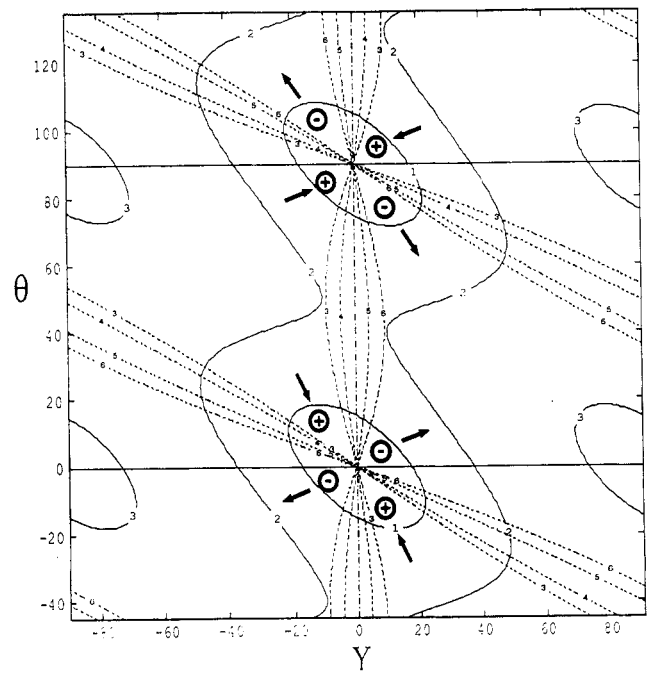


**Figure 12.** LD. This plot shows the very different effects of linear dichroism (multiple reflections give a similar map), in which the contours of highest and lowest fractional distortion extend over all of (Y, $\theta$) space. Note that the 'quadrupolar' symmetry of these distortions corresponds to a change in shape and orientation of the ellipse, but not to a displacement.

### *3.4. Effect of different parameters on the Δ trajectory of the 2D intensity minimum*

Figure 13 shows another graphical representation that has been very useful in classifying the effect of different wave-optic parameters. For a purely (linearly) birefringent material, the 2D minimum simply rotates with phase. When optical activity is introduced, the minimum position develops a 'trajectory', showing a singularity in its coordinates at $\Delta = (2n + 1)\pi$, the minimum position moving along the line $\theta = -\frac{1}{2}\Upsilon$.

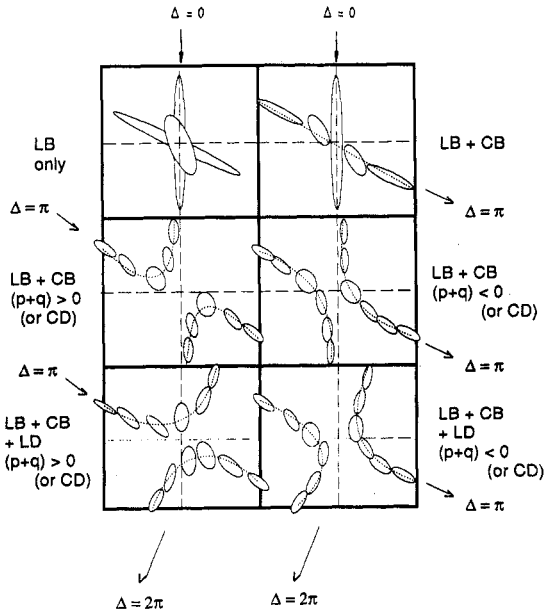


**Figure 13.** The behaviour of the orientation and position of the global 2D intensity minimum, $\Gamma(\Upsilon, \theta)$ as the phase is varied.

Parasitic ellipticity in the polariser and analyser produces another singularity at $\Delta = 2n\pi$, affecting the $\theta$-coordinate only by an amount related to the quantity $p + q$; $p - q$ works in a similar way to $k$, and circular dichroism in a similar way to $p + q$. Hence for an optically active birefringent section in a 'real' polarimeter we see two asymptotes, $\Upsilon = 0$, and $\theta = -\frac{1}{2}\Upsilon$.

We have already seen that linear dichroism distorts and rotates the intensity minimum; it also has a marked effect on the Δ trajectory. Both the $\Upsilon = 0$, and $\theta = -\frac{1}{2}\Upsilon$ asymptotes are rotated about the origin by angles that depend on the ratio between the linear dichroism and the linear birefringence.

## 4. Generalisation of the HAUP method

### *4.1. Non-dichroic, birefringent and optically active case*

Using the matrix notation introduced in section 2, the coefficients that give the intensity

for this case are

$$\mathbf{C} = \begin{bmatrix} (p+q)^2 + 4\sin^2(\Delta/2)[k^2 - k(p-q) - pq] & 2(p+q)\sin\Delta & 4\sin^2(\Delta/2) \\ -2(k-p)\sin\Delta & 4\sin^2(\Delta/2) & 0 \\ 1 & 0 & 0 \end{bmatrix}.$$

This can be refined in terms of five basis functions:

$$\Gamma = \Gamma \begin{bmatrix} 1 \\ \theta \\ \Upsilon\theta + \theta^2 \\ \Upsilon \\ \Upsilon^2 \end{bmatrix}.$$

It can be seen that the singular orientations and shapes of the HAUP map at $\Delta = 2n\pi$, and at $\Delta = (2n+1)\pi$ arise because of the equality and dependence on $\Delta$ of $C_{13}$ and $C_{22}$. The appearance of optical activity does not therefore alter these features, but rather introduces a displacive aspect to the singularity by means of $C_{21}$ and $C_{12}$.

*4.1.1. The $\theta'$-coordinate system.* An interesting feature of the above equation is that the nulling angle between crossed polars, defined by the condition

$$|\partial\Gamma/\partial\theta|_{\Upsilon=0} = 0 \qquad \text{when } \theta = \theta_0$$

is not at $\theta = 0$, but at $\theta = \theta_0$, where

$$\theta_0 = -\tfrac{1}{2}(p+q)\cot(\Delta/2).$$

This makes it impossible to determine the position $\theta = 0$ from the nulling angle. Recognising this, Kobayashi and Uesu transformed the equation for the intensity to the so-called $\theta'$-coordinate system, which has its origin at the nulling angle and can therefore be established experimentally. Referred to this coordinate system, the matrix of coefficients becomes

$$\mathbf{C} = \begin{bmatrix} (2k-\gamma)^2\sin^2(\Delta/2) & 0 & 4\sin^2(\Delta/2) \\ -(2k-\gamma)\sin\Delta & 4\sin^2(\Delta/2) & 0 \\ 1 & 0 & 0 \end{bmatrix}.$$

Here $\gamma = p - q$. The original HAUP method involves first making a separate measurement to establish the $\theta'$-coordinate system. Then, at various fixed $\theta'$, intensity readings as a function of $\Upsilon$ are taken and fitted to parabolae. The minima of these parabolae lie on a straight line in $(\Upsilon, \theta)$ space, gradient and intercept of which lead to $\sin^2(\Delta/2)$ and $2k - \gamma$.

We, on the other hand, use an improved method whereby a grid of intensity readings is taken relative to arbitrary $\theta$-coordinates and fitted by generalised linear least squares to a biquadratic polynomial in $\Upsilon$ and $\theta$. The $\theta_0$ transformation can then be performed 'automatically', by simply transforming the $\theta$-coordinates so that the coefficient of $\theta$

becomes zero, obviating the need for a separate measurement to determine $\theta_0$. This is a more correct procedure for two reasons. First, the answers do not hinge on a single measurement made to determine the position $\theta_0$. Second, by refining the grid as a whole rather than as a series of strips proper account is taken of correlations between the coefficients. The refinement yields the quantities $(2k - \gamma)\sin(\Delta)$ and $\sin^2(\Delta/2)$, from which $|(2k - \gamma)|$ and $|\Delta|$ can be derived.

*4.1.2. The γ-problem.* **If one is using a single grid, $k$ cannot be determined separately from $\gamma$. One of the solutions proposed by Kobayashi and Uesu was to exchange the** polariser and analyser, so that $\gamma$ becomes $-\gamma$, and repeat the measurement. Because $2k - \gamma$ is measured, $\gamma$ can in principle be eliminated. However, $\gamma$ is very sensitive to the exact alignment and position of the polariser and analyser prisms, and a method involving such a disturbance is unworkable—as pointed out by Kobayashi *et al* (1988). A more successful approach utilises a 'check' crystal with no optical activity to calibrate the instrument (Kobayashi *et al* 1988). Our solution, which does not involve any disturbance to the instrument, is to collect another grid with the crystal rotated by 90° about the

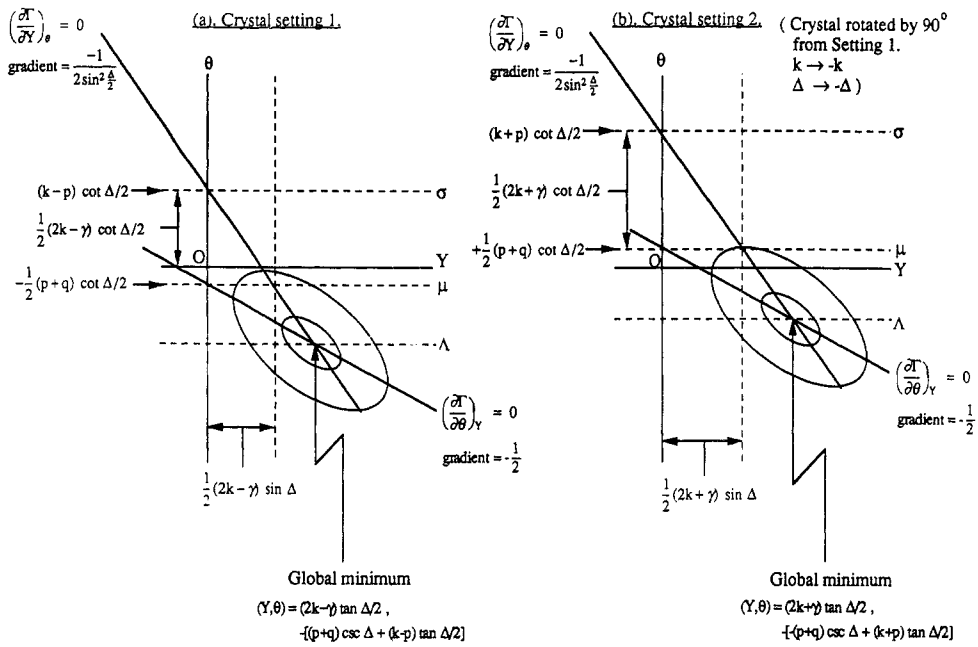


**Figure 14.** The two special crystal settings of our extended HAUP method, showing the way that $\gamma$ can be eliminated from the two readings. Indicated are the loci of the minima of the partial derivatives of $\Gamma$ with respect to Y and $\theta$. Also noted are the special azimuths of Szivessy and Münster. The geometrical significance of terms such as $(2k - \gamma)\sin\Delta$, which occur in the Kobayashi analysis, are indicated. In the crystal setting ($b$), the crystal has been rotated by 90°. This effectively causes a change of sign in both the phase and the normal-mode ellipticity. The expressions from the first setting are therefore replaced by those found when $\Delta$ is replaced by $-\Delta$, and $k$ by $-k$. This causes products such as $(2k - \gamma)\sin\Delta$ to undergo an apparent sign change in $\gamma$, which is operationally equivalent to leaving the crystal in the first setting but exchanging the polariser and analyser. Moving the crystal can, however, be done much more conveniently, and without any disturbance to the apparatus so long as the crystal microspositioning system is also capable of large and rapid movements.

beam direction. When the **M** matrix describing the crystal is appropriately transformed, $k$ is replaced by $-k$ and $\Delta$ by $-\Delta$ (the same happens to $k'$ and $E$ since this amounts simply to an exchange of the fast and slow directions). Since

$$[2(-k) - \gamma]\sin(-\Delta) = (2k + \gamma)\sin(\Delta)$$

we can again determine $k$ and $\gamma$ from the two grids (HAUP maps corresponding to the two crystal positions are shown in figure 14). Because no disturbance of the optical elements is involved, this is a significant improvement over both the other methods. We have found that the observed value of $\gamma$ depends critically on the temperature of the prisms, which in turn depends on beam heating, ambient temperature and so on. Our method has the additional advantage of speed, and so the measurements can be completed before significant temperature variation occurs.

*4.1.3. The $\delta$Y-error.* Kobayashi *et al* found divergences at certain values of $\Delta$ in their extracted value of $2k - \gamma$. They showed that these divergences could be explained if there were an error in the determination of the crossed-polar position. It was suggested that such an apparent '$\delta$Y' error could be caused by the imperfections in the prisms, and the surface of the sample not lying perpendicular to the beam. We have calculated the effect of both these suggestions. The former cannot give rise to a $\delta$Y error. We have calculated that the latter results in a very small effect for any realistic misalignment. Furthermore, this effect changes sign when the crystal is rotated by 90°, and hence could be eliminated in the same way as $\gamma$. The simplest way for the $\delta$Y-error to arise is of course if the motor drive for the polariser shows any drift during the course of the experiment. One technique we have employed with some success is to use the minimum of the HAUP map, for wavelengths at which $\Delta = 0$, to calibrate our Y-coordinates with the crystal *in situ*—this minimum should be at $Y = 0$ if the $\delta$Y-error is indeed only due to mechanical inaccuracies rather than the optical effects that Kobayashi postulated.

If a grid is refined in the presence of a $\delta$Y-error, the error in $2k - \gamma$ is given by

$$(2k - \gamma)_{\text{fitted}} = (2k - \gamma)_{\text{true}} - \delta Y \cot(\Delta/2)$$

and is sketched in figure 15.

### *4.2. Measurements in the presence of dichroism*

*4.2.1. Circular dichroism present but no linear dichroism.* If the assumption that $k' = 0$ is dropped, the untransformed matrix of coefficients becomes

$$\begin{bmatrix} (p+q)^2 + 4\sin^2(\Delta/2)[k^2 - k(p-q) - pq] & 2(p+q)\sin\Delta & 4\sin^2(\Delta/2) \\ \quad -2k'(p+q)\sin\Delta & \quad -8k'\sin^2(\Delta/2) & \\ -2(k-p)\sin\Delta - 4k'\sin^2(\Delta 2) & 4\sin^2(\Delta/2) & 0 \\ 1 & 0 & 0 \end{bmatrix}$$

The nulling angle is now given by

$$\theta_0 = -\tfrac{1}{2}(p+q)\cot(\Delta/2) + k'.$$

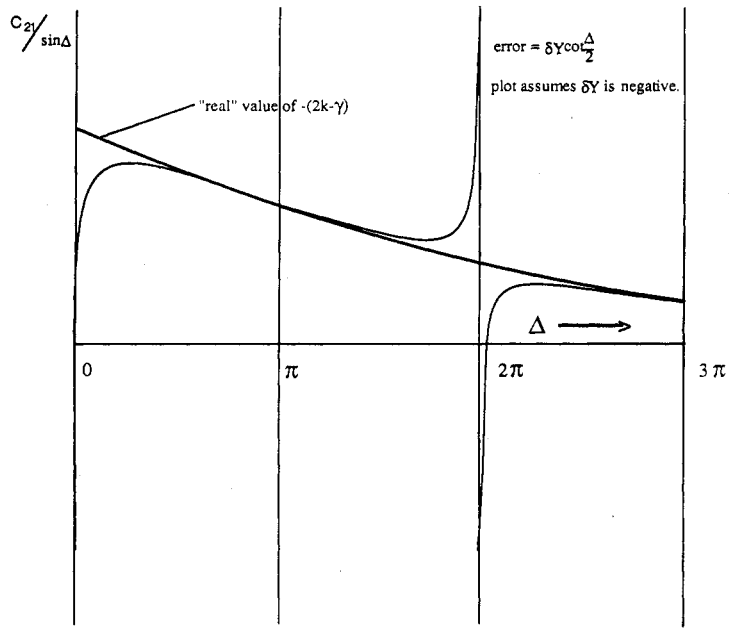


**Figure 15.** The effect of the $\delta$Y-error on the refinement of the parameter $2k - \gamma$.

The transformed matrix of coefficients is identical with that when there is no circular dichroism, except for the coefficient $C_{11}$ which is not used in the derivations of $2k - \gamma$ and $\Delta$. Therefore the $\theta_0$-transformation ensures that the determination of these quantities is unaffected by the existence of CD. To *measure* the CD it is necessary to use the fact that $k'$ appears in the expression for $\theta_0$. However, since our $\theta$-coordinates are arbitrary, we can only measure $\theta_e$, which differs from $\theta_0$ by an unknown additive constant which is independent of wavelength. Defining this constant angle as $\beta = \theta_e - \theta_0$ one has

$$\theta_e = -\tfrac{1}{2}(p + q)\cot(\Delta/2) + k' + \beta.$$

When $\Delta = (2m + 1)\pi\,(m = 0, 1, 2 \ldots)$ then $\theta_e = k' + \beta$. It is therefore possible straight away to determine $k'$ to within an additive constant at these special wavelengths, which in a sufficiently thick crystal can be relatively closely spaced. Furthermore, if one knows that the CD is zero except over a particular wavelength range (as would typically be the case when tracking through a CD band) it is possible to determine $\beta$ and hence the absolute magnitude of $k'$.

*4.2.2. Circular and linear dichroism present.* If $E \neq 0$ the untransformed matrix of coefficients becomes

$$\begin{bmatrix} (p+q)^2 + 4\sin^2(\Delta/2)[k^2 - k(p-q) - pq] & 2(p+q)\sin\Delta & 4\sin^2(\Delta/2) \\ \quad -2k'(p+q)\sin\Delta + \text{terms in } E & \quad -8k'\sin^2(\Delta/2) & \\ -2(k-p)\sin\Delta - 4k'\sin^2(\Delta/2) - 2k'E & 4\sin^2(\Delta/2) + 2E & 0 \\ 1+E & 0 & 0 \end{bmatrix}$$

Note that $C_{31}$ and $C_{22}$ are no longer equal; an extra basis function is required to refine the phase and the linear dichroism correctly, i.e. we must use the expression

$$\Gamma = \Gamma \begin{bmatrix} 1 \\ \theta \\ \theta^2 \\ \Upsilon \\ \Upsilon\theta \\ \Upsilon^2 \end{bmatrix}$$

decoupling the $\Upsilon\theta$ and the $\theta^2$-terms.
The nulling angle $\theta_0$ is, however, unaffected. The transformed matrix of coefficients is

$$\begin{bmatrix} (2k-\gamma)^2\sin^2(\Delta/2) & 0 & 4\sin^2(\Delta/2) \\ \quad + \text{other terms} & & \\ -(2k-\gamma)\sin\Delta & 4\sin^2(\Delta/2)+2E & 0 \\ \quad -E(p+q)\cot(\Delta/2) & & \\ 1+E & 0 & 0 \end{bmatrix}.$$

The $\theta_0$-transformation leaves terms involving $E$ in the coefficients $C_{12}$ and $C_{22}$, thus affecting the determination of $k$ and $\Delta$. This problem can be overcome as follows. It is easy to extract $E$ from the transformed $C_{ij}$—it is simply half the difference between the coefficients of $\theta^2$ and $\theta\Upsilon$.

$$E = \tfrac{1}{2}(C_{22} - C_{13}).$$

(The difference between these quantities can also be used to detect LD even when it is no longer small, although it is not possible then to refine out the other optical parameters.) However, the coefficient $C_{12}$ now contains an additional term

$$-E(p+q)\cot(\Delta/2).$$

In order to correct the extracted value of $2k-\gamma$ for this it is necessary to know $(p+q)\cot(\Delta/2)$—in practice, this means knowing the absolute value of $\theta_0$. This can be achieved by the method outlined in the section on circular dichroism, i.e. by measuring the nulling angle $\theta_e$ as a function of wavelength and producing a table of values of $(p+q)\cot(\Delta/2)$. These can then be combined with the fitted values of $E$ at each wavelength to produce correct values of $2k-\gamma$.

If a grid is refined on the false assumption that $E = 0$, then the fitted value of $2k-\gamma$ is given by

$$(2k-\gamma)_{\text{fitted}} = (2k-\gamma)_{\text{true}} + (p+q)E/\sin^2(\Delta/2)$$

as shown in figure 16.

Hence failure to allow for LD leads to divergences in the fitted value of $(2k-\gamma)$ at the same values of $\Delta$ as a '$\delta\Upsilon$'-error, although in the former case these are even functions of $\Delta$ and in the latter they are odd.

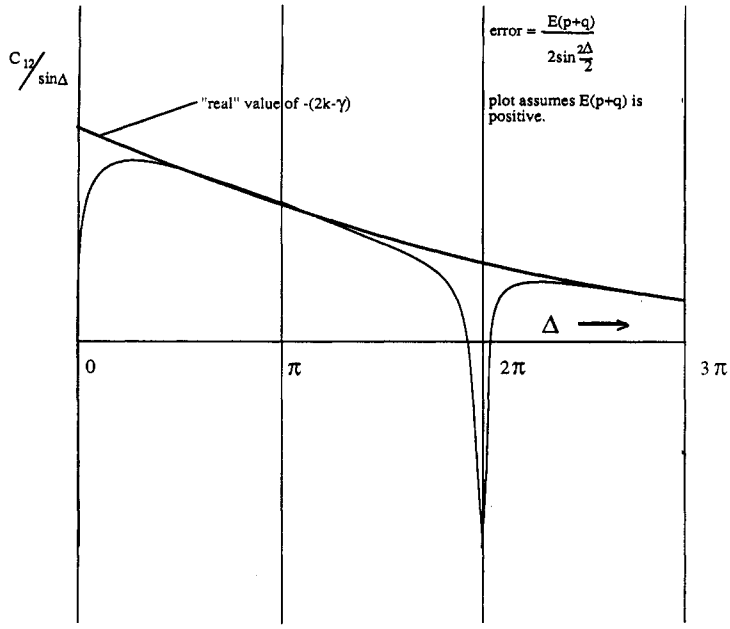


**Figure 16.** The effect of ignoring small but significant LD on the refinement of the parameter $2k - \gamma$.

Even a tiny amount of linear dichroism can have a significant effect on the intensity transmitted by the polarimeter. For example, consider a 1 mm thick sample of a material with a birefringence similar to that of quartz at a wavelength of 400 nm; this gives a value for the parameter $\delta = (\pi/\lambda)\Delta n \simeq 70\,000$. Even if the quantity $\varepsilon/\delta$ is as small as 0.001, then the parameter $E \simeq 0.2$, which is significant, especially at certain values of $\Delta$. Any material showing dispersion of its birefringence is in general linearly dichroic, by virtue of the Kramers–Kronig relationship connecting $\delta$ and $\varepsilon$. Furthermore, the presence of any source of anisotropic scattering, such as surface roughness, defects, strain, and the differential Fresnel reflection (due to the birefringence) will give rise to an effective LD that is not intrinsic to the pure material. The intrinsic contribution will be proportional to the crystal thickness and the surface contribution independent of it. Therefore two experiments on samples of different thickness will reveal the origins of the apparent LD. The effect of linear dichroism should certainly be considered even in crystals usually considered non-absorbing.

### *4.3. Multiple reflections*

At the interfaces between the crystal and the surrounding air there is inevitably some reflection, even at normal incidence, because of the difference in refractive indices between the media. Consequently the light is reflected back and forth between the crystal surfaces and the emergent light should be described by the Jones vector which is the sum of all these reflected beams. Following Melle (1985), this can be modelled by replacing the matrix **M** by **SM**, where **S** is calculated from the reflection matrix and from **M** itself. It is important to include the multiplicative phase factor in front of **M** for this purpose. For typical values of birefringence, the main contribution to **S** comes from the mean refractive index ($\bar{n}$), and the correction due to the birefringence is very small. It

is therefore sufficient to define a 'scalar reflection parameter' $r^2$:

$$r^2 = \left(\frac{1-\bar{n}}{1+\bar{n}}\right)^2 \cos\left(\frac{4\pi}{\lambda}\bar{n}z\right).$$

The matrix **SM** is similar in form to **M**, but is modified by terms depending on even powers of $r$. Retaining only the quadratic terms, the matrix of coefficients becomes

$$\begin{bmatrix} (p+q)^2+4\sin^2(\Delta/2)[k^2-k(p-q)-pq] & 2(p+q)\sin\Delta & 4\sin^2(\Delta/2) \\ \quad -2k'(p+q)\sin\Delta+\text{terms in } E & \quad -8k'\sin^2(\Delta/2) & \quad \times(1+2r^2) \\ -2(k-p)\sin\Delta-4k'\sin^2(\Delta/2) & 4\sin^2(\Delta/2) & 0 \\ \quad -2k'E(1-2r^2) & \quad \times(1+2r^2)+2E & \\ 1+E-2r^2\cos\Delta & 0 & 0 \end{bmatrix}.$$

Failing to include the effect of multiple reflections leads to an error in the determination of $\Delta$ given by

$$\{\sin(\Delta)\}_{\text{fitted}} = \{\sin(\Delta)\}_{\text{true}} \sqrt{1-4r^2\cos(\Delta)}.$$

This in turn leads to an error in the determination of $2k-\gamma$—in the worst case of about 8% (taking $n=1.5$). As the wavelength is changed this error shows a high-frequency component due to the dependence of $r$ on $\lambda$ and a lower-frequency component due to the variation of $\Delta$. The high-frequency oscillations will average to zero except in the very thinnest of the less strongly refringent samples.

### *4.4. Application to modulated methods*

All of the above analysis may easily be extended to cover modulated techniques such as that of Horinaka *et al.* The expression for the $2\omega$ Fourier component given earlier becomes

$$I_{2\omega} = I_0[(k-\varepsilon) - (k^2+\Theta^2)^{1/2}\cos(\delta+\zeta)]\sin\alpha$$

where $\varepsilon$ is an error term involving various combinations of $p$ and $q$, depending on the exact location of the experiment in $(\Upsilon, \theta)$ space. Whatever the setting, the parasitic ellipticities of the polariser and analyser may be eliminated by rotating the crystal through 90°. If the crystal is set at the crystallographic zero azimuth, then $\varepsilon = p$. If it is made to follow the minimal azimuth as the wavelength is changed (easily possible on our fully programmable polarimeter, to be described elsewhere), and the above equation is effectively $\theta_0$-transformed, then $\varepsilon = \gamma$ and the CD is conveniently eliminated, as in the Kobayashi experiment. Furthermore, there is no reason to limit the measurements to the position $(\Upsilon, \theta) = (0, 0)$ (as done by Horinaka *et al*)—much useful information is to be found at certain 'magic' positions such as $(0, \pi/4)$, or $(0, \pi/8)$ in which the optical activity and birefringence can be eliminated, and quantities such as the dichroisms can be seen on their own. Use can be made not only of the amplitude envelopes of the various Fourier components, but, at certain positions, also their phase envelopes. This will be the subject of a further paper.

## 5. Summary of the proposed method

(i) Set up the Y-coordinate system by making an accurate determination of the crossed-polar position, $Y = 0$.

(ii) Insert the crystal and with $Y = 0$ make measurements of the $\theta$-values of the nulling angles. From these it is possible to extract $k'$, the parameter describing the circular dichroism, and also $(p + q)\cot(\Delta/2)$ as a function of wavelength. This relies on the existence of a region in which the CD is zero.

(iii) Collect a series of grids relative to arbitrary $\theta$-coordinates and fit them to biquadratic polynomials. Transform each grid so that the coefficient of $\theta$ is zero and calculate $\Delta$ and $E$. Use the previously tabulated values for $(p + q)\cot(\Delta/2)$ in conjunction with $E$ to produce correct values for $2k - \gamma$.

(iv) Rotate the crystal by 90° and repeat (iii). Combine the results for $2k - \gamma$ and $2k + \gamma$ to produce $k$ and $\gamma$ separately.

## Acknowledgments

The authors would like to thank Professor J Kobayashi, Dr A M Glazer, Professor R M A Azzam, and Mr I Tebbutt for helpful discussions and Ms E E Williams and Mr F Wondre for the translation of papers written in French and German.

## Appendix 1. Outline of the least-squares method for refinement of the intensity surface $\Gamma(Y, \theta)$

(i) Transform data onto the ranges $\pm 1$ in $x$, $y$, and 0–1 in $z$, the intensity values.

(ii) Generate the weights $w_i = 1/\sigma_i^2$ where the standard deviation of a data point is calculated from the total photon count. Poisson counting statistics determine that if in a given time $N$ counts are received, then the standard deviation will be $N^{1/2}$. The photon detection system returns a count rate $R$, and counter values from which one can calculate an effective elapsed time (the so-called dead-time-corrected counting time, $\tau$)—hence:

$$\sigma(R) = \sqrt{R\tau'}/\tau' = \sqrt{R/\tau'}.$$

(iii) If we state the least-squares problem as $\alpha a = \beta$ where $\alpha = \mathbf{A}^T\mathbf{A}$, $\mathbf{A}$ is the design matrix, $a$ is the vector of parameters and $\beta = \mathbf{A}^T b$ where $b$ is the vector of weighted observations, then $a = \alpha^{-1}\beta$—we form $\alpha$ and $\beta$ in a triple summation, and sketch the outline of a program in pseudo-code:

```
For i = 1 to Number_of_DataPoints do
$(
  /* evaluate the coordinates x(i), y(i), the intensity z(i) and its weight w(i)
     from the raw photon counting data
  */

  x(i) = (raw_x(i) - x_centre)/x_half_range
  y(i) = (raw_y(i) - y_centre)/y_half_range
```

```
  z(i) = (raw_z(i) − z_min)/z_full_range
  w(i) = 1/σ²(i)

  /* then evaluate the basis functions */

  X1(x(i),y(i)) = ...
  X2(x(i),y(i)) = ...
      ...
  XNumber_of_Parameters(x(i),y(i)) = ...

  for k = 1 to Number_of_Parameters do
  $(
    β(k) = β(k) + w(i)X(k)z(i)
    for m = 1 to Number_of_Parameters do
      α(k,m) = α(k,m) + w(i)X(k)X(m)
  $)
$)
/*α and β are now formed. */

matrix_invert(α,α')
matrix_multiply(α',β,γ)        /* γ will now contain the parameters,
                                  and α', the inverse of α, will be the
                                  covariance matrix for the parameters.
                               */
```

## References


Anderson W J, Phil Won Yu and Park Y S 1974 *Opt. Commun.* **11** 392–5
Aspnes D E 1973 *Opt. Commun.* **8** 222–3
Azzam R M A 1978 *Optik* **52** 253–6
Baturin N A, Konstantinova A F, Perekalina Z B and Grechushnikov B N 1983 *Kristallografiya* **28** 503–9
Baturina O A, Okorochkov, Konstantinova A F, Perekalina Z B and Klimova A Y 1985 *Kristallografiya* **30** 715–9
Beaulard J 1893 Sur la coexistence du pouvoire rotatoire et de la double refraction dans le quartz *Thesis* Paris University.
Bruhat G and Grivet P 1935 *J. Physique Radium* **6** 12–26
Castaño F 1969 *Spectrochim. Acta* A **25** 401–5
Chetkin M V, Shevchuk L D and Ermilov N N 1979 *Sov. Phys.–Crystallogr.* **24** 223–5
Devarajan V and Glazer A M 1986 *Acta Crystallogr.* A **42** 560–9
Eimerl D 1988 *J. Opt. Soc. Am.* B **5** 1453–61
Glazer A M and Stadnicka K 1986 *J. Appl. Crystallogr.* **19** 108–22
Grechushnikov B N, Konstantinova A F, Lomako I D and Kalinkina I N 1980 *Sov. Phys.–Crystallogr.* **25** 346–8
Hearn A C 1985 *The Reduce User's Manual* (Santa Monica: Rand Corporation)
Henty D N and Jerrard H G 1976 *Surf. Sci.* **56** 170–81
Hobden M V 1968 *Acta Crystallogr.* A **24** 676
—— 1969 *Acta Crystallogr.* A **25** 633
Horinaka H, Sonomura H and Moyauchi T 1980 *Japan J. Appl. Phys. Suppl. 3* **19** 111–5
Horinaka H, Tomii K, Sonomura H and Miyauchi T 1985 *Jap. J. Appl. Phys.* **24** 755–60
Ivanov N R, Chikhladze O A 1976 *Kristallografiya* **21** 125–32
Ivanov N R and Konstantinova A F 1970 *Sov. Phys.–Crystallogr.* **15** 416
Jones R C 1948 *J. Opt. Soc. Am.* **38** 671

Kaminskii A A, Mill B V, Khodzhabagyan G G, Konstantinova A F, Okorochkov A I and Silvestrova I M 1983 *Phys. Status Solidi* a **80** 387
Kobayashi J, Asahi T and Takahashi S 1987 *Ferroelectrics* **75** 139–52
Kobayashi J, Asahi T, Takahashi S and Glazer A M 1988 *J. Appl. Crystallogr.* **21** 479–84
Kobayashi J, Bouillot J and Kinoshita K 1971 *Phys. Status Solidi* b **47** 619
Kobayashi J, Kumomi H and Saito K 1986a *J. Appl. Crystallogr.* **19** 337–81
Kobayashi J and Saito K 1986b *Proc. Japan. Acad.* **62** B 177–80
Kobayashi J, Takahashi T, Hosokawa T and Uesu Y 1978 *J. Appl. Phys.* **49** 809–13
Kobayashi J and Uesu Y 1983 *J. Appl. Crystallogr.* **16** 204–11
—— 1985 *Ferroelectrics* **64** 115–22
Kobayashi J, Uesu Y and Kumomi H 1984 *Phase Transitions* **4** 255–62
Kobayashi J, Uesu Y, Ogawa J and Nishihara Y 1985 *Phys. Rev.* B **31** 4569–75
Kobayashi J, Uesu Y J and Takehara H 1983 *J. Appl. Crystallogr.* **16** 212–9
Kong J A 1974 *J. Opt. Soc. Am.* **64** 1304–8
Konstantinova A F, Ivanov N R and Grechushnikov B N 1969 *Kristallografiya* **14** 283–92
Lakhtakia A 1985 *Appl. Phys.* B **36** 163–5
Melle H 1986 *Optik* **72** 157–64
Okorochkov A I, Konstantinova A F, Soboleva L V and Khapaeva L I 1984 *Kristallografiya* **29** 1102–8
Pancharatnam S 1955 *Proc. Indian Acad. Sci.* A **42** 86
Perekalina Z B, Kaldybaev K A and Konstantinova A F 1979 *Kristallografiya* **24** 847–50
Perekalina Z B, Kaldybaev K A, Konstantinova A F and Belyaev L M 1977 *Kristallografiya* **22** 556–61
Press W H, Flannery B P, Tenkolsky S A and Vetterling W T 1986 *Numerical Recipes* (Oxford: Oxford University Press)
Puri A and Birman J L 1981 *Opt. Commun.* **37** 81–3
Raab R E 1982 *Opt. Acta* **29** 1243–53
Ramachandran G N and Ramaseshan S 1961 *Handbuch der Physik* vol 25, ed S Flügge (Berlin: Springer)
Reijnhart R 1970 *Dissertation* Delft University
Saito K, Kawabe T and Kobayashi J 1987 *Ferroelectrics* **75** 153–66
Saito K, Kunishima I, Kobayashi J and Uesu Y 1985 *Ferroelectrics* **64** 137–44
Stetiu P 1983 *Surf. Sci.* **135** 276–83
Szivessy G and Münster C 1934 *Ann. Phys., Lpz.* **20** 703–36
Szivessy G and Schweers C 1929 *Ann. Phys., Lpz.* **5** 891
Vlokh O G, Klepatch N I and Shopa Y I 1986 *Ferroelectrics* **66** 267–74
Voigt W 1903 *Gottinger Nachr.* p 170
—— 1905 *Ann. Phys., Lpz.* **18** 645
Wever F 1920 *Jahrbuch der Philosophie* vol 2 (Gottingen: University Press) p 201 ff
Wyant J C 1981 *Appl. Opt.* **20** 3321–26